Eur. Phys. J. B (2017) 90: 249
DOI: 10.1140/epjb/e2017-80377-y

THE EUROPEAN PHYSICAL JOURNAL B

Regular Article

Second harmonic wave generation from Joule heating in layered organic conductors

Danica Krstovska[a] and Biljana Mitreska

Ss. Cyril and Methodius University, Faculty of Natural Sciences and Mathematics, Arhimedova 3, 1000 Skopje, Macedonia

Received 27 June 2017 / Received in final form 24 October 2017
Published online 13 December 2017 –

Abstract. The amplitude of a second harmonic wave (SHW) generated from Joule heating as a heat source in organic conductor β-(BEDT-TTF)$_2$IBr$_2$ is analyzed as a function of the magnetic field strength and its orientation with respect to the plane of the layers. Angular oscillations of the SHW amplitude are correlated with the angular changes of in-plane conductivity that arise from the periodic dependence of charge carriers velocity on the field orientation. It was found that the nonlinear effect of wave generation leads to a shift between the position of the peaks of the wave amplitude and in-plane conductivity. This allows an important information on the parameter values of organic conductors as well as wave velocity to be obtained. Magnetic field dependence shows that the wave is not strongly attenuated with increasing field and might give insights on the interactions between the electromagnetic, temperature and acoustic oscillations. We found that these observations are completely different compared to those of linear acoustic wave generation. It has been shown that the necessary conditions for observing the nonlinear acoustic wave generation are fulfilled in a wide range of fields and angles that allow the acoustic properties of organic conductors to be studied in detail.

1 Introduction

Ultrasonic nonlinear effects are the cause of the generation of higher harmonics in an acoustic wave propagating through a solid medium due to material nonlinearity. Usually, a source of nonlinearity in elastic wave propagation common to all materials is that from elastic nonlinearity, dislocations and micro-defects within the material. Nonlinear ultrasonics, including the investigation of higher harmonics caused by nonlinear material behavior, has proven to be a useful technique to investigate the condition of structural materials. Particularly, measuring the second harmonic provides a direct measure of the state of a material's microstructure (see Ref. [1] and references therein).

Another sources of nonlinearity are involved when the contactless generation of double frequency acoustic waves is considered. In the electromagnetic-acoustic conversion (EMAC) processes both the fundamental wave (FW) and higher harmonics can be generated. Therefore, there exist linear and nonlinear conversion mechanisms of EMAC. In the former, as far as the coupling between the electromagnetic and temperature oscillations is very weak a FW with frequency ω is generated. In the latter, the nonlinear effects in higher harmonics generation may arise from different causes such as the optical heating or an ac-current-induced Joule heating.

The mechanisms of linear transformation, which are responsible for generation of acoustic waves at the same frequency as the frequency of the electromagnetic wave ω that is incident on the surface of conducting media, are a standard subject of investigation in EMAC problems. The mechanism occurs as follows: when an electromagnetic wave with frequency ω is incident on the conductor, nonuniform temperature oscillations of the same frequency appear as a result of the thermoelectric effect. These oscillations, in turn, generate acoustic oscillations in the conductor with a frequency that coincides with the frequency of the incident electromagnetic wave (contactless excitation of acoustic waves). It has been shown that the inductive and deformation interactions are basically responsible for the linear generation of acoustic waves with frequency ω in isotropic metals [2–13] as well as in layered organic conductors [14,15]. Some theoretical and experimental studies in isotropic metals have shown that these mechanisms are also capable of generating acoustic oscillations with frequency 2ω, i.e., in the non-linear regime [16–19]. In the case of induction mechanism, the source of nonlinearity in the generation of double frequency acoustic wave is the action of the alternating magnetic field on the current it excites in the skin layer [16]. For the deformation mechanism of energy conversion, a source of nonlinearity is the nonlinear correction to the electron distribution function [18].

Apart from the induction and deformation forces, longitudinal acoustic waves at double frequency can also

[a] e-mail: danica@pmf.ukim.mk

be generated by other sources of nonlinearity. The most important such source is the force arising due to the appearance of thermoelastic stresses in the Joule heated skin layer [20]. The thermoelectric mechanism of acoustic wave generation is basically a nonlinear effect due to the action of the thermoelastic stresses on the crystal lattice. These stresses that are caused by the temperature oscillations with frequency 2ω ($\Theta \sim \cos(2\omega t)$) arising from the alternating part of the Joule heat generate an acoustic wave with double frequency 2ω, i.e., second harmonic wave (SHW). Joule heating is the characteristic of material that can be heated up when there is current flow because electrical energy is transformed into thermal energy. By far there is one published work that considers the linear acoustic wave generation in layered organic conductors (generation of a wave with fundamental frequency ω) due to thermoelectric effect [15] but the SHW generation has not been considered yet.

The purpose of the present work is to study the SHW generation and propagation in organic conductors under the action of thermoelastic stresses arising from the time dependent Joule heating. The quasi-two-dimensional (q2D) charge-transfer salts form the largest organic superconductor family with unusual normal and superconducting properties which come out of the layered structure as well as the specific shape of the Fermi surface. Their most remarkable feature is the reduced dimensionality of the electronic band structure caused by the specific character of their crystal structure [21]. This research considers the q2D organic conductor β-(BEDT-TTF)$_2$IBr$_2$, and tracks the SHW as a function of the magnetic field strength and its orientation. We find that studying the SHW properties can give important information not only about the parameters of the Fermi surface and electron energy spectrum of organic conductors but also about the interactions between the electromagnetic and temperature oscillations that are responsible for the wave generation. In the following we compare the properties of the FW and SHW generation and show that in organic conductors the SHW generation possesses different features compared to those of the FW. In layered organic conductors due to the small electron mean free-path the nonlinear wave generation could be studied in a wide range of magnetic fields and angles providing possibilities for experimental studies of SHW using non-contact ultrasonic techniques.

2 Theoretical model for second harmonic wave generation

Here we introduce the complete system of partial differential equations describing the SHW generation in organic conductors due to Joule heating. The current is applied at frequency $\omega = 10^8$–10^9 Hz, causing an oscillation of the temperature at frequency 2ω. We consider a case when electric currents, $\mathbf{j} = (0, j_y, 0)$, flowing through the conductor are along the less conducting axis, z-axis. Then the only nonzero component of the electric field is the y-component, $\mathbf{E} = (0, E_y, 0)$. The electric field induces thermoelectric stresses in the perpendicular direction, i.e., along the z-axis which in turn generate a longitudinal acoustic wave, $\mathbf{q} = (0, 0, q)$, of double frequency 2ω. Therefore all of the quantities in the equations presented below will depend only on the z-component. The conductor is placed in a magnetic field oriented at an angle θ from the normal to plane of the layers, $\mathbf{B} = (B\sin\theta, 0, B\cos\theta)$.

The SHW generation is manifested only under the conditions of the normal skin effect, when the electron mean-free path length l is much smaller than the skin depth of both the electromagnetic δ_E and thermal δ_T field in the conductor, $l \ll \delta_E, \delta_T$. The temperature Θ is a thermodynamically equilibrium characteristic of the state of a body. For this reason, a temperature oscillating with frequency 2ω ($\Theta \sim e^{-i2\omega t}$) can occur if $2\omega\tau \ll 1$ where τ is the relaxation time of the conduction electrons. In this case the condition for normal skin effect $k_T l \approx \sqrt{2\omega\tau} \ll 1$, where k_T is the thermal wave number, is satisfied automatically.

The necessary set of equations describing the SHW generation and propagation within the conductor concise of several partial differential equations:

Maxwell's equations for the magnetic $\mathbf{B}$ and electric $\mathbf{E}$ field

$$\mathrm{curl}\mathbf{B} = \mu_0 \mathbf{j}; \quad \mathrm{curl}\mathbf{E} = -\frac{\partial \mathbf{B}}{\partial t}, \tag{1}$$

the thermal conduction equation that describes the propagation of the acoustic wave with the presence of a heat flux $\mathbf{Q}$ and a heat source J_h

$$C\frac{\partial \Theta}{\partial t} + \mathrm{div}\mathbf{Q} = J_h, \tag{2}$$

the equation of heat flux

$$Q_i = -\kappa_{ik}\frac{\partial \Theta}{\partial x_k}, \tag{3}$$

the equation of the theory of elasticity for ionic displacement $\mathbf{U} = (0, 0, U)$ that takes into account the thermoelectric stress tensor

$$\rho\frac{\partial^2 U_i}{\partial t^2} - \lambda_{iklm}\frac{\partial U_{lm}}{\partial x_k} = \rho s^2 \beta \delta_{ik}\frac{\partial \Theta}{\partial x_k}. \tag{4}$$

Here μ_0 is the magnetic permeability of the vacuum, Θ is the high-frequency addition to the mean temperature T of the crystal, J_h is the power density of the heat source, C is the volumetric heat capacity, κ_{ik} is the thermal conductivity tensor, ρ and λ_{iklm} are the density and elastic tensor of the crystal and β is the volumetric expansion coefficient. The subscripts in U and x describe the acoustic wave polarization and direction of propagation, respectively.

The above system of equations must be supplemented with the corresponding boundary conditions for Maxwell's equations, heat flux and wave amplitude at the conductor's surface. The boundary conditions for Maxwell's equations are continuity of the tangential components of the electric and magnetic fields. In the case when the source of thermoelastic stresses is the time-dependent part

of Joule heating the boundary condition for the heat flux reduces to the requirement that there is no heat flux through the surface

$$Q_{zz} = \kappa_{zz}\frac{\partial\Theta}{\partial x}|_{z=0} = 0. \tag{5}$$

The boundary condition for the equation of elasticity

$$\frac{\partial U}{\partial z}|_{z=0} = -\beta\Theta|_{z=0}, \tag{6}$$

is a consequence of the non-specular nature of the scattering of electrons by the conductor's surface.

Under the conditions of normal skin effect, the relation between current density $\mathbf{j}$ and electric field $\mathbf{E}$ is local to a high degree of accuracy, $\mathbf{j} = \sigma\mathbf{E}$. Using Maxwell's equations one obtains the following expression for the Joule heating dissipation

$$J_h = \frac{j_y^2}{\sigma_{yy}} = -\frac{k^4}{\omega^2\mu_0^2}\frac{1}{\sigma_{yy}}e^{2i(kz-\omega t)}, \tag{7}$$

where

$$k = \frac{1+i}{\delta_E} \text{ and } \delta_E = \sqrt{\frac{2}{\omega\mu_0\sigma_{yy}}}, \tag{8}$$

are the wavenumber and skin depth of the electromagnetic field, respectively.

Consequently, equations (2)–(4) take the following form:

$$-2i\omega C\Theta + \frac{\partial Q_z}{\partial z} = J_h, \tag{9}$$

$$Q_z = -\kappa_{zz}\frac{\partial\Theta}{\partial z}, \tag{10}$$

$$\frac{\partial^2 U_{2\omega}}{\partial z^2} + q^2 U_{2\omega} = \beta\frac{\partial\Theta}{\partial z}, \tag{11}$$

where s and $q = 2\omega/s$ are the SHW velocity and wave vector, respectively.

Substituting equations (7) and (10) in equation (9) we obtain the following expression for the temperature distribution within the conductor

$$\frac{\partial^2\Theta}{\partial z^2} + k_T^2\Theta = \frac{\sigma_{yy}}{4\kappa_{zz}}e^{2i(kz-\omega t)}, \tag{12}$$

where

$$k_T = \frac{1+i}{\delta_T} \text{ and } \delta_T = \sqrt{\frac{\kappa_{zz}}{\omega C}}, \tag{13}$$

are the wavenumber and skin depth of the thermal field under the conditions of a normal skin effect.

Crucial part in further theoretical analysis is to obtain the solutions of equation (12) and substitute them in equation (11) for the amplitude of the generated SHW to be determined.

The solution $\Theta(z)$ that satisfies the boundary condition equation (5) is given as

$$\Theta(z) = \frac{\sigma_{yy}}{4\kappa_{zz}}\frac{e^{2ikz} - \frac{2k}{k_T}e^{ik_T z}}{k_T^2 - 4k^2}. \tag{14}$$

By substituting equation (14) in equation (11) we obtain the following solution for the SHW amplitude

$$U_{2\omega} = \frac{\beta\sigma_{yy}}{2\omega qC}\frac{k_T}{k_T+2k} \times\left(1 + \frac{2kk_T(q^2 - q(k_T+2k) + 2kk_T)}{(q^2-4k^2)(q^2-k_T^2)}\right). \tag{15}$$

The components of the conductivity tensor σ_{ij} which relate the current density to the electric field, $j_i = \sigma_{ij}E_j$, can be calculated by using the Boltzmann transport equation for the non-equilibrium correction Ψ to the equilibrium electron distribution function $f_0(\varepsilon)$, based on the tight binding approximation band structure within the single relaxation time approximation τ [22]

$$\frac{\partial\Psi}{\partial t_B} + \frac{\Psi}{\tau} = e\mathbf{E}\mathbf{v}, \tag{16}$$

where t_B is the time motion of the conduction electrons in a magnetic field and e is the charge of conduction electrons. The interlayer thermal conductivity component κ_{zz} is obtained by means of electrical conductivity σ_{zz} as follows [22]

$$\kappa_{zz} = \frac{\pi^2 k_B^2 T}{3e^2}\sigma_{zz}, \tag{17}$$

where k_B is the Boltzmann constant. The solution of the Boltzmann transport equation

$$\Psi_i = eE_i\int_{-\infty}^{t} dt' v_i(t')e^{\frac{t'-t}{\tau}}, \tag{18}$$

determines the components of the electrical conductivity tensor

$$\sigma_{ij} = \frac{2e^3B}{(2\pi\hbar)^3}\int\frac{\partial f_0}{\partial\varepsilon}d\varepsilon\int dp_B\int_0^{T_p} dt v_i(t)\Psi_j. \tag{19}$$

Here $\hbar$ is the Planck's constant divided by 2π and $T_p = 2\pi/\omega_c$ is a period of motion of electrons in a magnetic field with cyclotron frequency $\omega_c = eB\cos\theta/m^*$. m^* is the electron's effective mass.

The SHW generation is analyzed for layered organic conductors with a simplified q2D electron energy spectrum of the form

$$\varepsilon(p) = \frac{p_x^2 + p_y^2}{2m^*} - \eta\frac{v_F\hbar}{c}\cos\frac{cp_z}{\hbar}, \tag{20}$$

where η is the quasi-two dimensionality parameter, v_F is the Fermi velocity of the electrons in the plane of the layers and c is the interlayer spacing (along the z-axis).

In the main approximation in the small parameter η the expressions for the interlayer conductivity σ_{zz} and in-plane conductivity σ_{yy} take the following form

$$\sigma_{zz} = \sigma_0 \left(\cos\theta J_0^2 \left(\frac{cD_p}{2\hbar} \tan\theta \right) + \frac{\gamma^2}{B^2} + \tan^2\theta \left(\frac{\gamma^2}{B^2} + \eta^2 \right) \right), \quad (21)$$

and

$$\sigma_{yy} = \frac{\gamma^2 \sigma_0}{B^2} + \tan^2\theta \left(\frac{\gamma^2 \sigma_0}{B^2} + \sigma_{zz} \right), \quad (22)$$

where σ_0 is the electrical conductivity along the layers in the absence of a magnetic field, $D_p = 2p_F$ is the averaged diameter of the Fermi surface along the p_x-axis, J_0 is the zeroth order Bessel function and $\gamma = m^*/e\tau$.

3 Results and discussion

The SHW amplitude $U_{2\omega}$ is a function of the frequency of applied electric current (electric field) ω, the magnetic field B, the angle between the normal to the layers and the magnetic field θ as well as of the kinetic characteristics of the q2D conductor (interlayer and in-plane conductivity).

In the following, we shall analyze the amplitude $U_{2\omega}$ as a function of the magnetic field strength and its orientation with respect to the layers plane. The parameter values chosen to obtain the amplitude $U_{2\omega}$ are for the quasi-two dimensional organic conductor β-(BEDT-TTF)$_2$IBr$_2$ although calculations can be used to obtain the field and angular behavior of the SHW amplitude for other organic conductors such are β-(BEDT-TTF)$_2$I$_2$Br and $\beta_{\rm H}$-(BEDT-TTF)$_2$I$_3$ as they are isostructural and have similar electronic properties with β-(BEDT-TTF)$_2$IBr$_2$. Their Fermi surface consists of a corrugated cylinder open in the direction of the normal to the layers. For β-(BEDT-TTF)$_2$IBr$_2$, the quasi-two dimensionality parameter is taken to be $\eta = 0.01$, the electron's effective mass is $m^* = 4.2m_e$ and the relaxation time is $\tau = 10\,\text{ps}$ [21].

3.1 Angular second harmonic wave oscillations (ASHWO)

The angular oscillations are characteristic of the kinetic and thermoelectric coefficients of layered organic conductors and are associated with the charge carriers motion on the cylindrical Fermi surface in a tilted magnetic field. They arise from the periodic dependence of the average electron velocity v_z of the conduction electrons on the angle θ. Since the amplitude $U_{2\omega}$ is determined by the in-plane and interlayer electrical conductivity, σ_{yy} and σ_{zz} (as seen from Eq. (15)), it is expected the angular second harmonic wave oscillations (ASHWO) to emerge when a constant magnetic field is turned from the direction normal to conducting layers toward the plane of the layers. Consequently, a similarity between the ASHWO and the conductivity can be expected from the Boltzmann transport theory.

When the vectors $\mathbf{q}$ and $\mathbf{B}$ are not orthogonal, the average velocity of charge carriers in the direction of wave propagation differs from zero at the cylindrical Fermi surface, i.e., charge carriers drift in the direction of wave propagation. The existence of points at which the interaction with the wave is most effective on different trajectories leads to a resonant dependence of the acoustic wave amplitude on magnetic field B and the angle between the normal to the layers and magnetic field θ.

Figure 1 shows the resonant oscillations of the SHW amplitude $U_{2\omega}$ on the angle θ for several field values with pronounced peaks (maximum $U_{2\omega}(\theta)$) and dips (minimum $U_{2\omega}(\theta)$) at certain angles whose height increases with increasing angle θ. The amplitude $U_{2\omega}(\theta)$ is very sensitive to the magnetic field orientation with tilting the field from the z-axis (that is normal to the layers and, hence, parallel to the axis of the Fermi cylinder) toward a direction parallel to the layers.

When thermal waves, and consequently acoustic waves, are generated by applying an ac current across a conductor, the amplitude of both the thermal and acoustic wave is related to the electrical conductivity (resistivity) of the conductor. In this regard, in order to understand the SHW generation and propagation in organic conductors we first analyze the angular oscillations of interlayer and in-plane conductivity (inset of Fig. 1). For arbitrary magnetic field direction θ the Bessel function $J_0(cD_p \tan\theta/2\hbar)$ is generally nonzero. When $\tan\theta > 1$ electrons may execute many orbits before dephasing, resulting in the resonance. In that case, the first term in equation (21) for the interlayer conductivity σ_{zz}, is dominant. For $\tan\theta \gg 1$ this term becomes negligible when the angle $\theta = \theta^{\min}$ satisfies the condition $\frac{cD_p}{2\hbar} \tan\theta^{\min} = \pi(n - \frac{1}{4})$ where n is an integer [23,24]. For these values of θ the zeroth-order Bessel function $J_0(cD_p \tan\theta^{\min}/2\hbar)$ equals to zero. This leads to a vanishing averaged velocity $\bar{v}_z$ and, hence, minimum interlayer conductivity. For other values of θ satisfying the condition $\frac{cD_p}{2\hbar} \tan\theta^{\max} = \pi(n + \frac{1}{4})$, the z-component of the Fermi velocity is maximum, $\bar{v}_z^{\max} \simeq 2\eta v_F$, which gives rise to a local maximum in the interlayer conductivity. The in-plane conductivity $\sigma_{yy}(\theta)$ also exhibits strong oscillations as expected since it is determined by the interlayer conductivity (see Eq. (22)), but with much stronger amplitude (see inset in Fig. 1). In addition, the positions of the peaks in the $\sigma_{yy}(\theta)$ dependence are slightly shifted toward larger angles form the peaks of $\sigma_{zz}(\theta)$ due to the strong anisotropy in the layered organic conductors. For the organic conductor β-(BEDT-TTF)$_2$IBr$_2$, this shift is of order of 0.001 that corresponds to the conductivity anisotropy ratio in this compound, $\sigma_\perp/\sigma_{||} \sim 10^{-3}$ ($\sigma_\perp$ and $\sigma_{||}$ are the resistivities across and within the layers, respectively [21]).

It is instructive to discuss our results on the SHW generation in organic conductors in the context of previous results on the linear thermoelectric generation

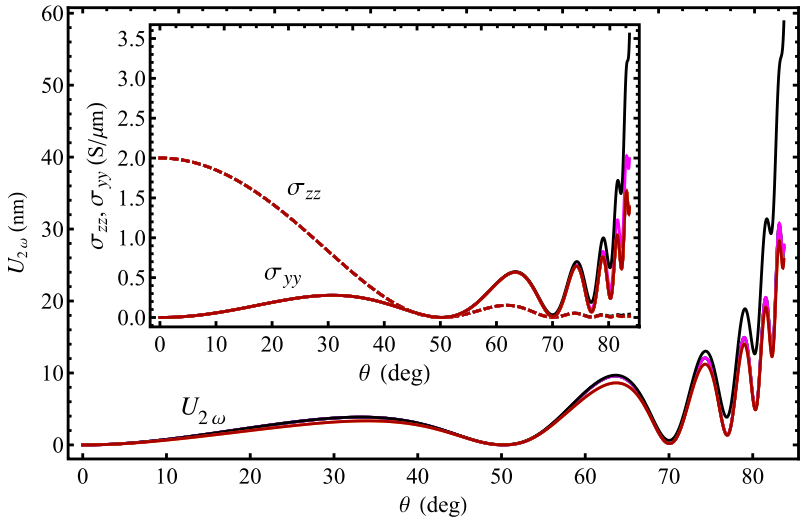

Fig. 1. Angular dependence of the SHW amplitude $U_{2\omega}$ for $T = 20\,\mathrm{K}$, $\eta = 0.01$ and several field values $B = 0.8$, 1.5, 3, 6, 8, 10, 12, 15 and 20 T from top to bottom. The inset shows the angular oscillations of the in-plane $\sigma_{yy}(\theta)$ (solid curves) and interlayer electrical conductivity $\sigma_{zz}(\theta)$ (dashed curves) for the same η, T and B.

of fundamental acoustic waves (with frequency ω) [15]. Our findings reveal several important aspects of distinct behavior of the FW and SHW in organic conductors with the magnetic field strength and its orientation with respect to the plane of the layers. We first note that the FW excited through thermoelectric mechanism the amplitude U_ω is determined by the interlayer electrical conductivity and thermoelectric power of the conductor. It was shown that the position of the peaks in the angular oscillations of FW amplitude U_ω coincide with the position of the extremes in the angular oscillations of interlayer conductivity σ_{zz} [15].

As shown in Figure 1, we find in the present work that in organic conductors the angular oscillations of the SHW amplitude $U_{2\omega}(\theta)$ resemble those of the in-plane conductivity $\sigma_{yy}(\theta)$. In the vicinity of angles where the amplitude $U_{2\omega}(\theta)$ has maximum value, $\theta_{\mathrm{max}i}$ $(i = 1, 2, 3, 4, 5)$ (Fig. 2), the average drift velocity of charge carriers along the acoustic wavevector $\bar{v}_z$ coincides with the wave velocity s, and therefore their interaction with the wave is most effective. As a result, at these angles the amplitude is the largest (especially this trend is apparent for $\theta > 50°$) and $U_{2\omega}(\theta)$ exhibits peaks in the angular dependence.

An important feature to emphasize is that the position of the peaks of $U_{2\omega}(\theta)$ do not coincide to those of $\sigma_{yy}(\theta)$ but are found to be shifted toward larger angles for $\Delta\theta$ (see Fig. 2). This confirms that the temperature rise due to Joule heating is at a different harmonic than the temperature rise due to thermoelectric effect which allows for independent observation of the waves. The shift decreases with increasing angle and contains an important information about the Fermi surface corrugation and electron energy spectrum. As θ approaches 90°, when the magnetic field approaches the orientation parallel to the layers, there is almost no shifting between the position of the peaks. This can be ascribed to the suppression of the angular oscillations due to the more elongated elliptic orbits in which an electron fails to perform a complete revolution during the mean free time. Also, with tilting the field from the z-axis, the drift of charge carriers along the z-axis, $\bar{v}_z$, decreases but the drift along the y-axis, $\bar{v}_y = v_F + \bar{v}_z \tan\theta$, is rather large at angles close to $\theta = 90°$.

The behavior observed suggests that the difference between the FW and SHW properties could be related to the different correlations between electromagnetic and thermal oscillations that affect the generation and propagation of the waves. The FW is generated due to thermoelectric effect through a linear process when the coupling between the electromagnetic and temperature oscillations is very weak. This, on the other hand, means that the FW is transmitted within the conductor by the thermal wave which dissipates at distance proportional to the thermal skin depth δ_T. Experimentally, the observation of the effect by reflection could be difficult except at lower temperatures when the thermal skin depth is much larger than the electromagnetic skin depth ($\delta_T \gg \delta_E$). As regards the SHW, it is generated through a nonlinear process when the coupling between the electromagnetic and temperature oscillations can be significant due to the large local temperature gradients generated by the Joule heating. As expected from the Joule heating property, when a current is applied to the conductor, the surface immediately starts to heat up which results in a local increase of temperature due to the thermal power dissipation. When a current is driven through the conductor, dissipation related to Joule effect is greatest along the direction with the greatest resistance which in the present case is along the direction of the SHW propagation (z-axis). Due to the nonlinearity correlated with the large thermal dissipation there could be a peculiar "pulling" of the electromagnetic wave by the thermal wave which causes a phase difference between the SHW amplitude and in-plane conductivity. However, the absence of significant shift at large angles suggests that the SHW properties are not determined only by the thermal characteristics of the conductor but can

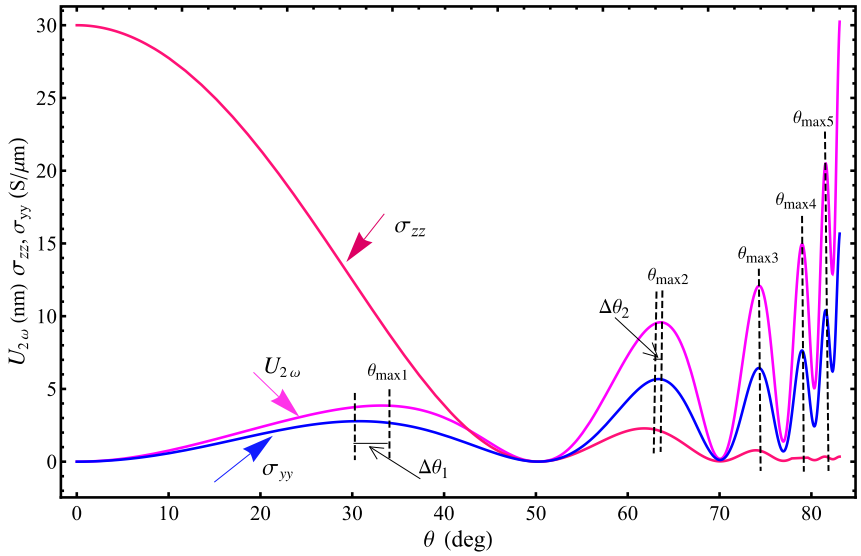

Fig. 2. Angular dependence of the SHW amplitude $U_{2\omega}(\theta)$, interlayer conductivity σ_{zz} and in-plane conductivity σ_{yy} for $T = 20\,\mathrm{K}$, $\eta = 0.01$ and $B = 1.5\,\mathrm{T}$. The angles $\theta_{\mathrm{max}i}$ $(i = 1, 2, 3, 4, 5)$ correspond to the maximum value of the SHW amplitude and $\Delta\theta_i$ $(i = 1, 2)$ indicate the shift between the position of the peaks in the angular oscillations of the SHW amplitude $U_{2\omega}(\theta)$ and in-plane electrical conductivity $\sigma_{yy}(\theta)$ for the first and second peak in the $U_{2\omega}(\theta)$ dependence observed at $\theta_{\mathrm{max1}} = 33.26^\circ$ and $\theta_{\mathrm{max2}} = 63.61^\circ$, respectively. The $\sigma_{zz}(\theta)$ and $\sigma_{yy}(\theta)$ curves are scaled for clarity.

also be attributed to the electrodynamic characteristics, i.e., the transmission of the SHW is conditioned not only by the thermal wave (as in the case of FW) but also by the electromagnetic wave. This is further discussed below in more detail by taking into account the magnetic field and angular dependence of both the electromagnetic and thermal skin depth.

From the shift between the peaks of $U_{2\omega}(\theta)$ and $\sigma_{yy}(\theta)$ the value of the quasi-two dimensionality parameter η and thus the interlayer transfer integral $t_c = 2\eta\varepsilon_F$ in the electron energy spectrum (Eq. (20)) of β-(BEDT-TTF)$_2$IBr$_2$ can be calculated. Indeed, a rough estimate gives that the shift in θ positions is $\Delta\theta \sim 4\eta^2 \tan\theta$, i.e., is angle dependent. From the shift around the first peak, $\theta_{\mathrm{max1}} = 33.26^\circ$ (Fig. 2), we find that $\eta = 0.018$. Given the value of η and Fermi energy $\varepsilon_F = 0.1\,\mathrm{eV}$ [21] we estimate that for β-(BEDT-TTF)$_2$IBr$_2$ the transfer integral along the z-axis is of the order of $t_c = 0.36\,\mathrm{meV}$ which fits well with the one extracted from data on magnetic quantum oscillations $t_c = 0.35\,\mathrm{meV}$ [21].

For $U_{2\omega}$ plotted versus $\tan\theta$ (Fig. 3), the same trends are apparent, where the positions of the minima are indicated as $\theta_{\mathrm{min}i}$ $(i = 1, 2, 3, 4, 5, 6)$. The positions of the peaks and dips in the SHW amplitude are unaffected by magnetic field strength and repeat periodically in the scale of $\tan\theta$. We present the amplitudes of both the FW and SHW (inset in Fig. 3) to further address distinct features in generation of both waves. For the FW amplitude we make use of the calculations presented in reference [15] and apply the parameter values for β-(BEDT-TTF)$_2$IBr$_2$ as in the present work.

The comparison between amplitudes shows that the amplitude of the FW exceeds by far the one of the SHW. This is expected as thermal waves, and hence acoustic waves, decay more rapidly when they travel at higher frequencies. Indeed, with increasing frequency the electromagnetic and thermal skin depth decrease which in turn leads to a generation of acoustic waves with smaller amplitude. Exception are certain angles ($\tan\theta_{\mathrm{min}i}$, $i \geq 3$ in Fig. 3) where the SHW amplitude is larger than the one of the FW. For $\tan\theta \gg 1$ the minima in the $U_{2\omega}(\tan\theta)$ dependence do not correspond to zero SHW amplitude as in the case of $U_{\omega}(\tan\theta)$ dependence for the FW amplitude. While for the former the value of amplitude at the peaks is close to that in minima (especially at larger angles), in the latter the amplitude of acoustic oscillations is increasing with increasing angle and the value of the amplitude at the peaks is much larger than the one at the minima. This indicates that $U_{\omega}(\tan\theta)$ exhibits giant angular oscillations that are not characteristic for the SHW amplitude implying that the interaction of charge carriers with both waves will be effectively different for different angles θ. For the FW the drift velocity $\bar{v}_z$ of charge carriers along the acoustic wavevector coincides with the wave velocity s only in the vicinity of the peaks where their interaction with the wave is most effective. In the case of SHW, $\bar{v}_z^{\max} = s$ in the vicinity of angles $\theta = \theta_{\max}$ but also $\bar{v}_z^{\max} \sim s$ in the vicinity of angles $\theta_{\min}$ meaning that the charge carriers interact more effectively with the SHW in the whole range of angles. This allows the SHW velocity s to be determined by using that $\bar{v}_z^{\max} \simeq 2\eta v_F$. The Fermi velocity of β-(BEDT-TTF)$_2$IBr$_2$ is $v_F = 1.5 \times 10^5\,\mathrm{m/s}$ [25] which gives $s \simeq 6000\,\mathrm{m/s}$.

Another important feature to emphasize is that with increasing magnetic field the $U_{2\omega}(\theta)$ curves are close to each other (especially for $B \geq 6$ T). This is clearly seen from $\tan\theta$ dependence in Figure 3. Below $\tan\theta = 3$, the $U_{2\omega}(\tan\theta)$ curves tend to overlap at any magnetic field and for $\tan\theta > 3$, $U_{2\omega}(\tan\theta)$ curves are slightly shifted downward (SHW is weakly attenuated) with increasing

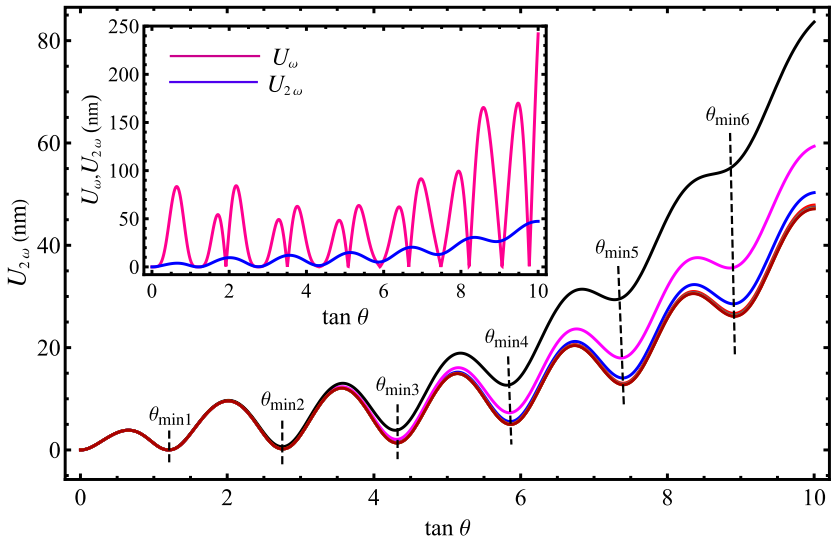

Fig. 3. $\tan\theta$ positions of the SHW amplitude $U_{2\omega}$ for $T = 20\,\mathrm{K}$, $\eta = 0.01$ and the same field values as in Figure 1. The position of the minima in the $U_{2\omega}(\tan\theta)$ dependence are given by the angles $\theta_{\mathrm{min}i}$ $(i = 1, 2, 3, 4, 5, 6)$. The inset shows the $\tan\theta$ dependence of the FW amplitude U_ω and SHW amplitude $U_{2\omega}$ for the same η, T and $B = 10\,\mathrm{T}$.

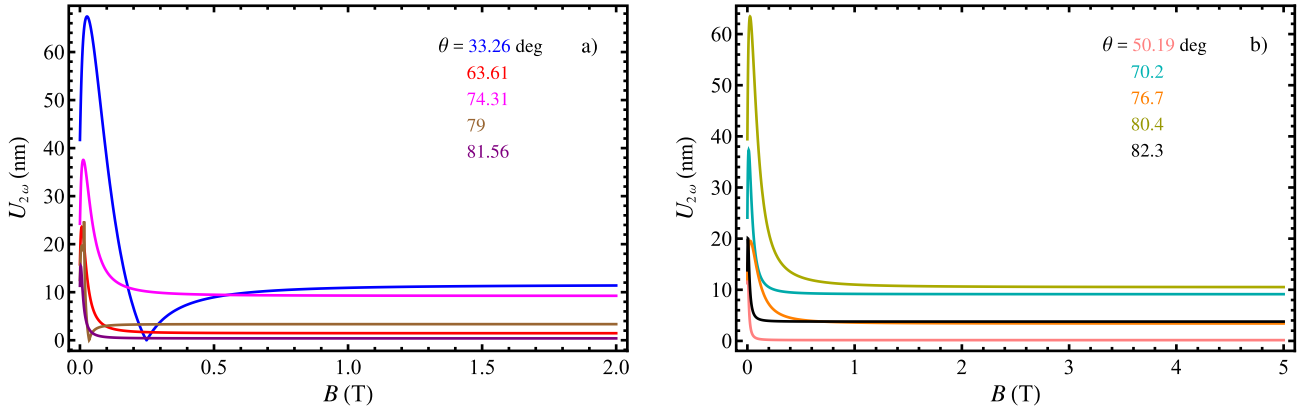

Fig. 4. Magnetic field dependence of the second harmonic amplitude $U_{2\omega}(B)$ for $\eta = 0.01$, $T = 20\,\mathrm{K}$ and several field directions from the normal to the layers that correspond to the maxima (a) $\theta_{\mathrm{max}} = 33.26°, 63.61°, 74.31°, 79°, 81.56°$ and minima (b) $\theta_{\mathrm{min}} = 50.19°, 70.2°, 76.9°, 80.4°, 82.3°$ angles of the SHW angular oscillations in Figure 2.

field. This indicates that the inductive mechanism which is due to the Lorentz force acting on the conduction electrons, $F_L = j_y B \sin\theta$, does not affect much the SHW amplitude. It is possible that the induction force is compensated with the large thermal dissipation induced due to Joule effect. This is quiet opposite from the case of FW generation where for larger magnetic fields the wave is strongly attenuated, and the inductive mechanism dominates over the thermoelectric one [15].

3.2 Magnetic field dependence of SHW amplitude

Figure 4 shows the magnetic field dependence of SHW amplitude $U_{2\omega}(B)$ in β-(BEDT-TTF)$_2$IBr$_2$ for $T = 20\,\mathrm{K}$ and several field directions from the normal to the layers that correspond to the maximum ($\theta_{\mathrm{max}} = 33.26°$, $63.61°$, $74.31°$, $79°$, $81.56°$) and minimum ($\theta_{\mathrm{min}} = 50.19°$, $70.2°$, $76.9°$, $80.4°$, $82.3°$) SHW amplitude in the angular dependence in Figure 2.

Independently on whether the field is tilted at the maximum or minimum angle, the SHW generation starts at zero magnetic field and is most effective at low fields. With increasing field the SHW is attenuated but not as strongly as the FW which attenuates at lower fields, $B = 0.6\,\mathrm{T}$ [15]. Above the maximum value the amplitude $U_{2\omega}(B)$ decreases in proportion to B^{-1} reaching a weakly field dependence with increasing field. This behavior is correlated with the magnetic field dependence of both the electromagnetic and thermal skin depth. Usually high-frequency properties of the layered organic conductors are quite sensitive to the polarization and direction of propagation of electromagnetic field in the plane of the layers. In order to further analyze the field behavior of the SHW amplitude and determine how it changes with the thermal and electrodynamic characteristics of the conductor we present in Figure 5 the electromagnetic and thermal skin depth, δ_E and δ_T, plotted as a function of the magnetic field at angles that correspond to maximum and minimum

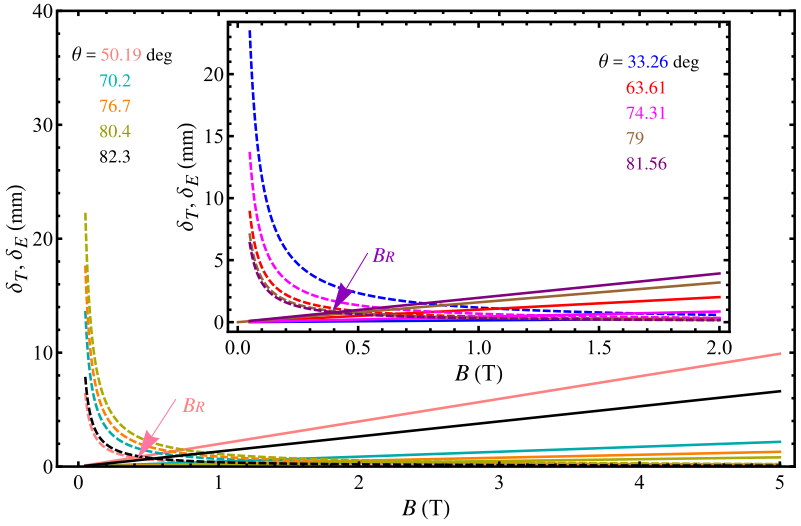

Fig. 5. Magnetic field dependence of the electromagnetic δ_E (solid curves) and thermal δ_T (dashed curves) skin depth for $\eta = 0.01$, $T = 20\,\mathrm{K}$ and the same field directions from the normal to the layers as in Figure 4. The magnetic field B_R that corresponds to the resonance condition is indicated for $\theta_{\mathrm{min1}} = 50.19°$ and $\theta_{\mathrm{max5}} = 81.56°$.

SHW amplitude. Following the changes in skin depths with field and angle allows to distinguish if the SHW generation is determined by the thermal or electrodynamic characteristics of the conductor.

The electromagnetic skin depth is linear in field, i.e., increases with the magnetic field in proportion to B^1, $\delta_E(B) \sim \frac{B}{\gamma(1+\tan^2\theta)}(\frac{2}{\omega\mu_0\sigma_0})^{1/2}$. On the other hand, the thermal skin depth $\delta_T(B) \sim \frac{\gamma}{B}\left(\frac{\sigma_0(1+\tan^2\theta)}{\omega C}\right)^{1/2}$ decreases with increasing field in proportion to B^{-1}. At low fields, around the peak in the $U_{2\omega}(B)$ dependence, and angles up to $\theta = 40°$, the thermal skin depth is larger than the electromagnetic skin depth, $\delta_T > \delta_E$ because in this range of fields and angles the interlayer conductivity is larger than the in-plane conductivity as evident from Figure 2. In that case the SHW is transmitted by the thermal wave and $U_{2\omega}(B)$ decreases with increasing field as $\delta_T(B)$, i.e., approximately in proportion to B^{-1}. Our results show that with further increasing angle the electromagnetic and thermal skin depth become equal at certain field B_R that is angle dependent, $\delta_T = \delta_E$, that corresponds to a resonance between electromagnetic and temperature (acoustic) oscillations. A possible reason for the resonance is that in the process of nonlinear acoustic wave generation when the coupling between electromagnetic and temperature oscillations is not negligible, a part of the heat source energy remains in the electromagnetic wave which dissipates at distance $\sim \delta_E$. This could cause a "pulling" of the electromagnetic wave by the thermal wave which in turn leads to a shift between the position of the peaks of the SHW amplitude and in-plane conductivity. In addition, we suggest that the resonance between the oscillations does not allow the SHW to be strongly attenuated with increasing field as in the case of FW. For $\theta > 50°$ and above B_R, the electromagnetic skin depth is larger than the thermal one, $\delta_E > \delta_T$, and the SHW properties are conditioned by the electrodynamic characteristics of the conductor. This is however expected as in this range of angles the in-plane conductivity is larger than the interlayer conductivity. The weak field dependence of $U_{2\omega}(B)$ above B_R is ascribed to the small changes in δ_E with field. In the case of a linear wave generation due to the weak coupling the thermal skin depth is always larger than the electromagnetic one and the FW is transmitted mainly by the thermal wave that dissipates at distance $\sim \delta_T$.

3.3 Possibilities for experimental studies of SHW generation in organic conductors

The SHW generation due to Joule heating as a heat source is constraint by the condition $2\omega\tau \ll 1$. In the organic conductor β-(BEDT-TTF)$_2$IBr$_2$ this condition is always fulfilled, even at high frequencies, $\omega = 10^8$–$10^9\,\mathrm{Hz}$, as the relaxation time of charge carriers τ is very small ($\tau = 10\,\mathrm{ps}$). In addition, for the generation of waves to be the most effective other conditions must be satisfied. This includes fulfillment of $q\delta_T \ll 1$ as long as the conditions for normal skin effect $l \ll \delta_E, \delta_T$ are satisfied. A Fermi velocity of $v_F = 1.5 \times 10^5\,\mathrm{m/s}$ gives an electron mean free-path of order of $l = v_F\tau = 1.5\,\mu\mathrm{m}$. We have obtained from Figure 5 the following values (depending on the angle) for the electromagnetic and thermal skin depth at $B = 1\,\mathrm{T}$, $\delta_E = 0.14$–$1.9\,\mathrm{mm}$ and $\delta_T = 0.32$–$1.2\,\mathrm{mm}$, respectively. It is evident that the electron mean free-path is much smaller than both skin depths providing the SHW generation to be studied experimentally in a wide range of magnetic fields and angles. Experiments on SHW generation in layered organic conductors would be highly favorable since these compounds are synthesized with high purity that makes them very convenient for performing experiments. Studying the SHW generation in organic conductor will allow detection of crystal imperfections such as microcracks or cavities, which are often met in organic metal crystals. It is more important that the investigation of

SHW can give additional information about the unusual properties of the layered organic conductors. For example, the magnetic field and angular dependences of the in-plane electrical conductivity σ_{yy} can be revealed through how SHW amplitude changes with field and angle which could be very useful since measurements of σ_{yy} are typically much less reliable than the measurements on the interlayer conductivity σ_{zz}. Also, the angular oscillations of the SHW allow the characteristic parameters of the Fermi surface to be determined such as the quasi-two dimensionality parameter η which determines the corrugation of the Fermi surface of the material. In addition, the transfer integral t_c in the electron energy spectrum as well the SHW velocity s can be estimated from the angular measurements that do not require high magnetic fields. Furthermore, studying the SHW generation could reveal detailed information about the coupling between electromagnetic, thermal and acoustic oscillations in layered organic conductors.

Although the layered organic conductor β-(BEDT-TTF)$_2$IBr$_2$ is a simple system, i.e., the model of the simplest energy spectrum for the charge carriers is considered, it allows, in many cases, a correct understanding of the electron transport and dynamics in layered organic conductors. The resonance response in the SHW generation as observed here can be used as a solid tool for probing different materials, in particular the multilayered structures of organic origin. Recently, the second-order nonlinear plasmon excitations for gapped graphene were investigated in context of second harmonic generation [26]. It was shown that there is an order of magnitude enhancement of the second harmonic generation resonance with growing gap. The formalism presented in reference [26] could be applied to investigate the SHW generation in multilayered structures of organic origin such as the q2D organic conductor α-(ET)$_2$KHg(SCN)$_4$ that has a substantial gap near the Fermi level. In addition, the authors suggest that the formalism is an alternative to dc induced enhancement in second harmonic generation but without underlying anisotropy induced by the current. This is especially important to take into account when the object of investigation is the gapped multilayered organic conductors as they are characterized as highly anisotropic systems.

4 Conclusions

The nonlinear generation of acoustic waves of double frequency 2ω ($\omega = 10^8$–10^9 Hz) in layered quasi-two dimensional organic conductors due to Joule heating as a heat source is considered. Only a SHW is generated due to the thermoelectric stresses caused by the alternating part of the Joule heat and its amplitude is analyzed as a function of the magnetic field B, the angle θ between the normal to the layers and the magnetic field as well as of the conductor's characteristics. Specifically, the parameter values for the organic conductor β-(BEDT-TTF)$_2$IBr$_2$ are used to obtain the SHW amplitude $U_{2\omega}$ at $T = 20$ K and $\eta = 0.01$, i.e., for not strongly warped cylindrical Fermi surface. We find that the oscillatory dependence of the SHW amplitude $U_{2\omega}$ is determined mainly by the angular oscillations of the in-plane conductivity and are associated with the periodic charge carriers motion on the cylindrical Fermi surface in a tilted magnetic field. At angles where $U_{2\omega}$ is maximum, the average drift velocity of charge carriers along the wave vector coincides with the wave velocity s. Therefore narrow peaks appear in the angular dependence of $U_{2\omega}$ that correspond to the most effective interaction of the charge carriers with the wave. It has been also shown that the positions of the peaks of the SHW angular oscillations are shifted from those of the in-plane conductivity. This is attributed to the pulling of the electromagnetic wave by the thermal wave due to the coupling between electromagnetic and temperature oscillations. The shift allows important parameters that define the Fermi surface and electron energy spectrum of organic conductors to be estimated. Following the magnetic field dependence of the SHW as well as electromagnetic and thermal skin depth a valuable information on the interaction between electromagnetic and thermal oscillations can be obtained. This will allow to determine if the SHW generation and transmission within the conductor is conditioned by the thermal or electromagnetic field. In addition, a comparison between the linear and nonlinear acoustic wave generation reveals that both phenomena show completely different features resulting from the distinctive heat source. We suggest that the investigation of the SHW generation is of greater interest than the FW generation not only for studying the acoustic properties of organic conductors but also for determining the coupling parameters between the electronic and ionic subsystems. In layered organic conductors due to the small electron mean free-path the nonlinear wave generation can be observed in a wide range of magnetic fields and angles providing possibilities for experimental studies that will give new insights into the unusual electronic properties of these systems.

Author contribution statement

All the authors have equal contribution. All the authors have read and approved the final manuscript.

References

1. K.H. Matlack, J.Y. Kim, L.J. Jacobs, J. Qu, J. Nondestruct. Eval. **34**, 273 (2015)
2. V.M. Kontorovich, A.M. Glushyuk, Zh. Eksp. Teor. Fiz. **41**, 1195 (1961)
3. V.Ya. Kravchenko, Zh. Eksp. Teor. Fiz. **54**, 1494 (1968)
4. V.L. Fal'ko, Zh. Eksp. Teor. Fiz. **85**, 300 (1983) [Sov. Phys. JETP **58**, 175 (1983)]
5. A.N. Vasil'ev, Yu.P. Gaidukov, M.I. Kaganov et al., Fiz. Nizk. Temp. **15**, 160 (1989)
6. G. Turner, R.L. Thomas, D. Hsu, Phys. Rev. B **3**, 3097 (1971)
7. W.D. Wallace, M.R. Gaerttner, B.W. Maxfield, Phys. Rev. Lett. **27**, 995 (1971)

8. D.E. Chimenti, C.A. Kukkonen, B.W. Maxfield, Phys. Rev. B **10**, 3228 (1974)
9. D.E. Chimenti, Phys. Rev. B **13**, 4245 (1976)
10. N.C. Banic, A.W. Overhauser, Phys. Rev. B **16**, 3379 (1977)
11. E.A. Kaner, V.L. Fal'ko, L.P. Sal'nikova, Fiz. Nizk. Temp. **12**, 831 (1986)
12. E. Kartheuser, S. Rodriguez, Phys. Rev. B **33**, 772 (1986)
13. M.A. Gulvanskii, Fiz. Tverd. Tela **29**, 1249 (1987)
14. O. Galbova, G. Ivanovski, D. Krstovska, Low Temp. Phys. **29**, 939 (2003)
15. D. Krstovska, O. Galbova, T. Sandev, Europhys. Lett. **81**, 37006 (2008)
16. I. Cap, Acta Phys. Slov. **32**, 77 (1982)
17. A.P. Korolyuk, V.I. Khizhnyi, JETP Lett. **48**, 385 (1988)
18. A.N. Vasil'ev, M.A. Gulyanskii, M.I. Kaganov, Zh. Eksp. Teor. Fiz. **91**, 202 (1986)
19. N.M. Makarov, F.P. Rodriguez, V.A. Yampol'skii, Zh. Eksp. Teor. Fiz. **95**, 205 (1988)
20. L.D. Favro, IEEE Ultrason. Symp. Proc. **1**, 399 (1986)
21. M.V. Kartsovnik, Chem. Rev. **104**, 5737 (2004)
22. A.A. Abrikosov, *Fundamentals of the theory of metals*, 2nd edn. (North-Holland, Amsterdam, 1988)
23. K. Yamaji, J. Phys. Soc. Jpn. **58**, 1520 (1989)
24. R. Yagi, Y. Iye, T. Osada, S. Kagoshima, J. Phys. Soc. Jpn. **59**, 3069 (1990)
25. A. Chernenkaya, A. Dmitriev, M. Kirman, O. Koplak, R. Morgunov, Solid State Phenom. **190**, 615 (2012)
26. G. Gumbs, Y. Abranyos, U. Aparajita, O. Roslyak, AIP Conf. Proc. **1590**, 143 (2014)